

Electronic Supplementary information

Colloidal bimetallic platinum-ruthenium nanoparticles in ordered mesoporous carbon films as highly active electrocatalysts for the hydrogen evolution reaction

René Sachse ^{a,b}, Denis Bernsmeier ^a, Roman Schmack ^a, Ines Häusler ^c, Andreas Hertwig ^b,
Katrín Kraffert ^a, Jörg Nissen ^d, and Ralph Kraehnert ^{*a}

^a Technische Universität Berlin, Faculty II Mathematics and Natural Sciences, Institute of Chemistry, Straße des 17. Juni 135, 10623 Berlin, Germany

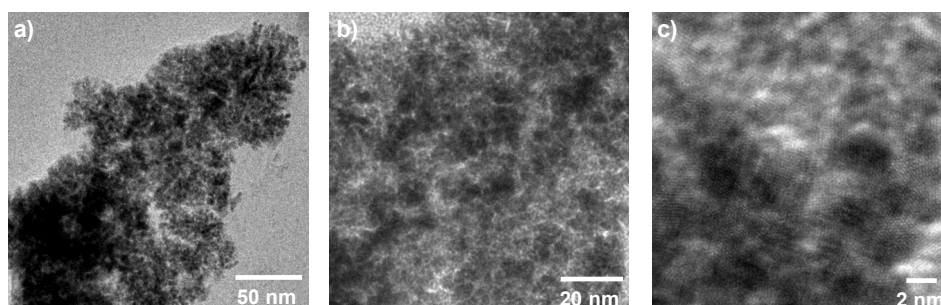
^b Federal Institute for Materials Research and Testing (BAM), Unter den Eichen 44-46, 12203 Berlin, Germany

^c Technische Universität Berlin, Faculty II Mathematics and Natural Sciences, Institute of Optics and Atomic Physics, Straße des 17. Juni 135, 10623 Berlin, Germany

^d Technische Universität Berlin, ZELMI, Straße des 17. Juni 135, 10623 Berlin, Germany

SI 1. Influence of colloidal particle synthesis parameter

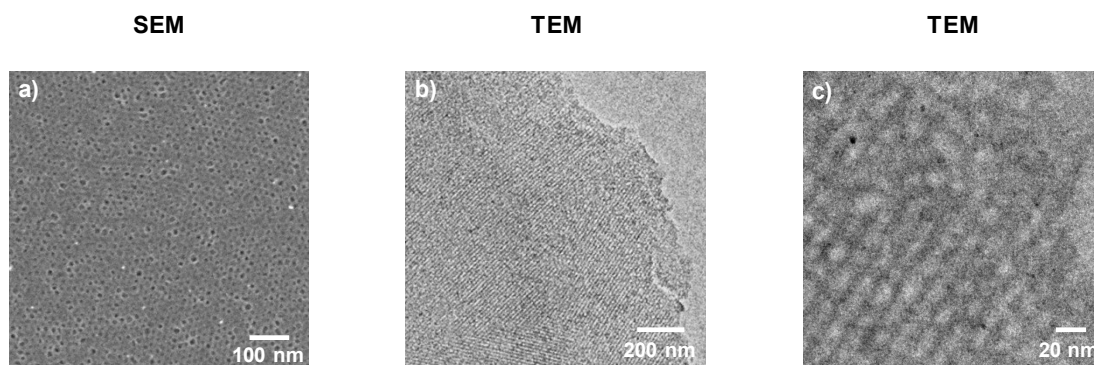
Colloidal ruthenium nanoparticles were synthesized using ruthenium acetylacetonate ($\text{Ru}(\text{acac})_3$) as RuNP precursor and tetraoctylammonium hydridotriethylborat as reducing and stabilization agent. TEM images of these particles (figure S1) indicate a strong agglomeration of the particles due to the absence of stabilization of the ammonia ligand.



Supplementary Figure S1: TEM images of colloidal ruthenium nanoparticles from nanoparticle synthesis using the $\text{N}(\text{octyl})_4\text{BEt}_3\text{H}$ agent and $\text{Ru}(\text{acac})_3$ as precursor.

SI 2. SEM / TEM images of the Pt_{0.06}Ru_{0.94}NP/OMC film

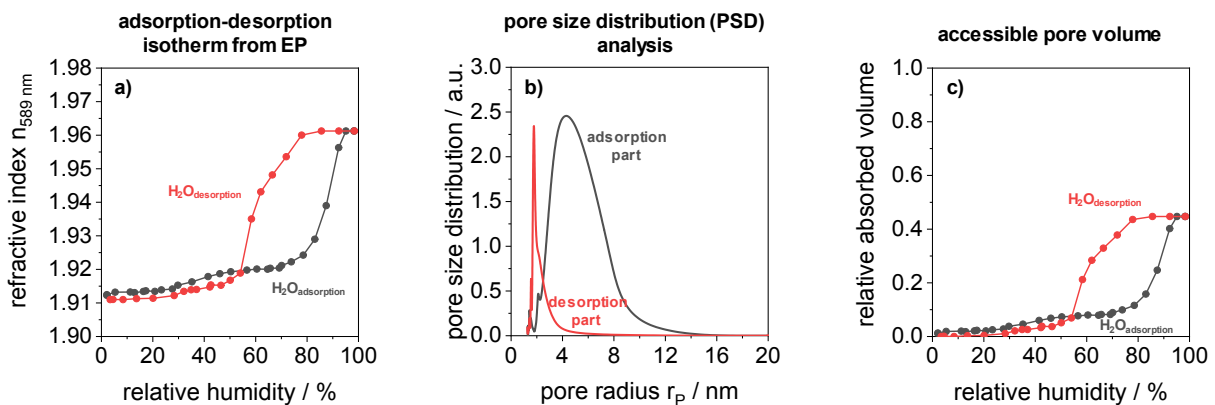
SEM and TEM images of the ordered mesoporous carbon film with integrated platinum-ruthenium nanoparticles (Pt_{0.06}Ru_{0.94}NP/OMC). SEM top-view image (a) show ordered pore openings at the outer surface. TEM images (b and c) of a film fragment indicate the mesopore structure throughout the film volume.



Supplementary Figure S2: SEM and TEM images of Pt_{0.06}Ru_{0.94}NP/OMC film. a) SEM image in top-view mode which indicates the ordered mesopore structure of the film. b) and c) present TEM images of a fragment from the Pt_{0.06}Ru_{0.94}NP/OMC film which show the ordered mesopore structure throughout the film volume.

SI 3. Pore size and pore volume evaluation by Ellipsometric Porometry (EP)

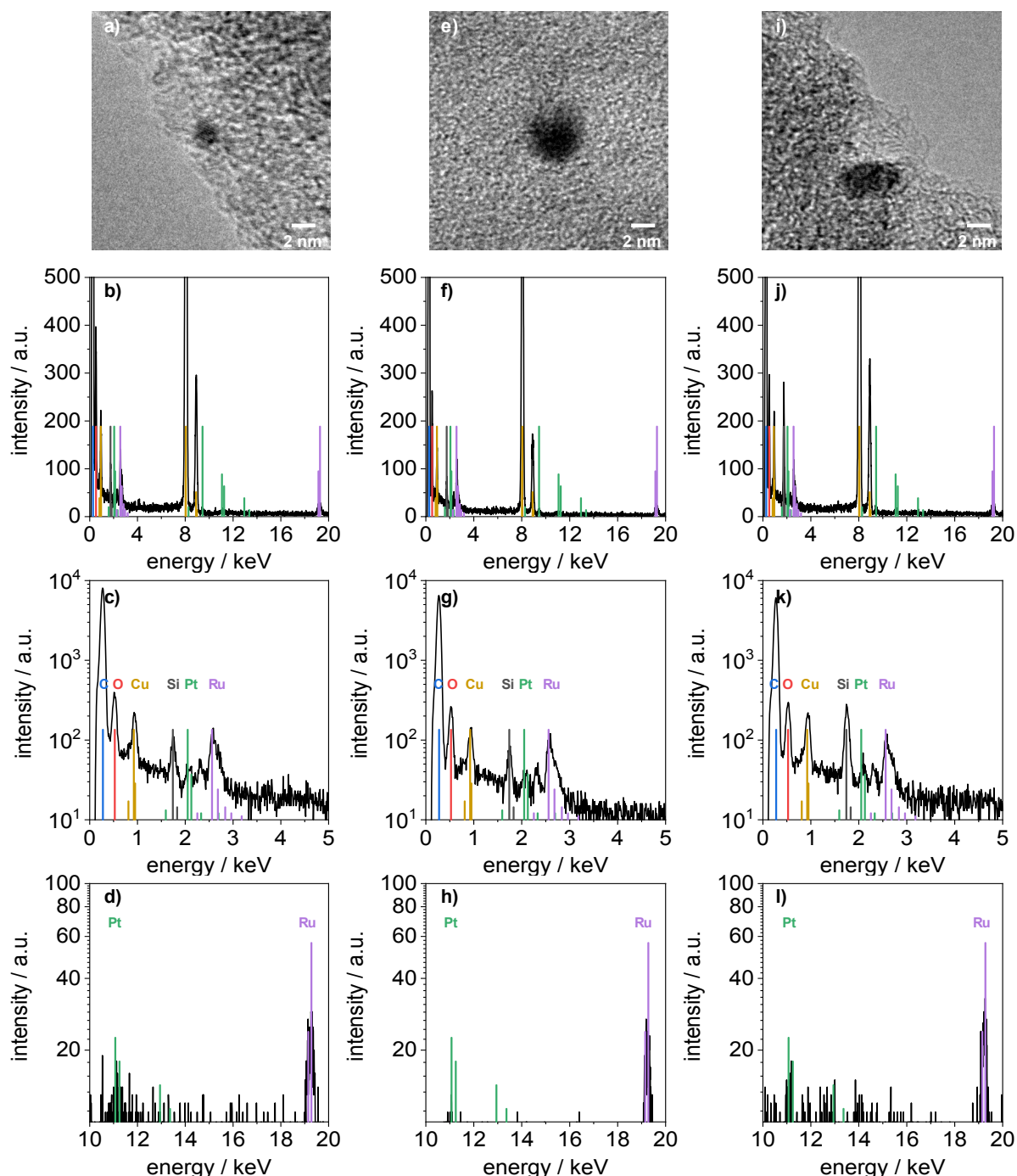
A pore size distribution (PSD) is obtained from an adsorption-desorption isotherm of an Ellipsometric Porometry (EP) measurement employing water as adsorbate (S3). The relative humidity is altered by mixing dry N_2 gas with N_2 gas saturated with water. The overall flow rate was 2.5 L min^{-1} . The PSD is calculated via a modified Kelvin equation considering the anisotropy of the mesopores by an anisotropic Bruggeman effective medium approximation (EMA). The anisotropic factor gives a Kelvin geometric factor G of 1.65 (for spherical pores G is 2 and for slit-like pores G becomes nearly 1). Similar values are described for films with a cubic mesopores structure in literature.¹ An untemplated carbon film is used to determine the thickness of water adsorbed on the surface at each r.H. The contact angle θ of the mesoporous film amounts to 67.5° .



Supplementary Figure S3: Ellipsometric Porosimetry (EP) analysis of a mesoporous carbon film with integrated platinum-ruthenium nanoparticles (0.3 wt%_{Pt} and 2.2 wt%_{Ru}) carbonized at 700 °C in H₂/Ar and additionally heat-treated at 300 °C in air and reduced in H₂/Ar at 350 °C. a) adsorption-desorption isotherm employing wet N₂-gas (flow rate 2.5 L min⁻¹). b) pore size distribution from the hysteresis of the adsorption isotherm. c) accessible pore volume derived from the employed calculation model.

SI 4. Single point TEM-EDX analysis

Single point TEM-EDX analyses of small nanoparticle are shown in Supplementary figure S4. The EDX spectra indicates for each nanoparticle the presence of a small Pt signal for the Pt M α and L α lines. Due to the low amount of Pt (0.06 $\mu\text{g cm}^{-2}$) the EDX intensity is very low and a quantification not feasible.

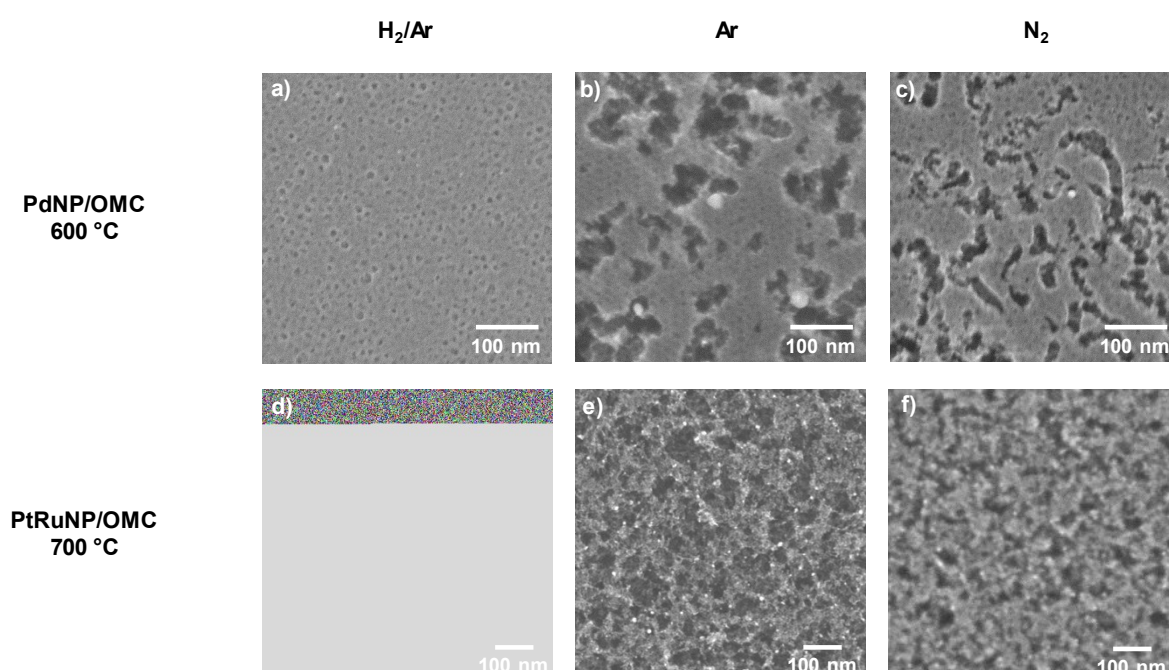


Supplementary Figure S4: Single point TEM and EDX analyses of small particle of a fragment of the Pt_{0.06}Ru_{0.94}NP/OMC film. a), e) and i) are HR-TEM images of the analyzed particles. b), f) and j) presents the EDX spectra of the shown particles. c), g) and k) show the logarithmic plots of the EDX spectra in the range of 0 - 5 keV and d), h) and l) the logarithmic plots in the range of 10 - 20 keV.

SI 5. Influence of the atmosphere during carbonization

The influence of the carbonization atmosphere was investigated by treating mesoporous carbon films with integrated palladium nanoparticles (PdNP) and platinum-ruthenium alloy nanoparticles (PtRuNP) in different atmospheres during carbonization. PdNP/OMC films were carbonized in a tube furnace at 600 °C for 3 h in H₂/Ar-atmosphere, Ar-atmosphere as well as in N₂-atmosphere and PtRuNP/OMC films at 700 °C for 3 h in H₂/Ar-atmosphere and Ar-atmosphere(S5).

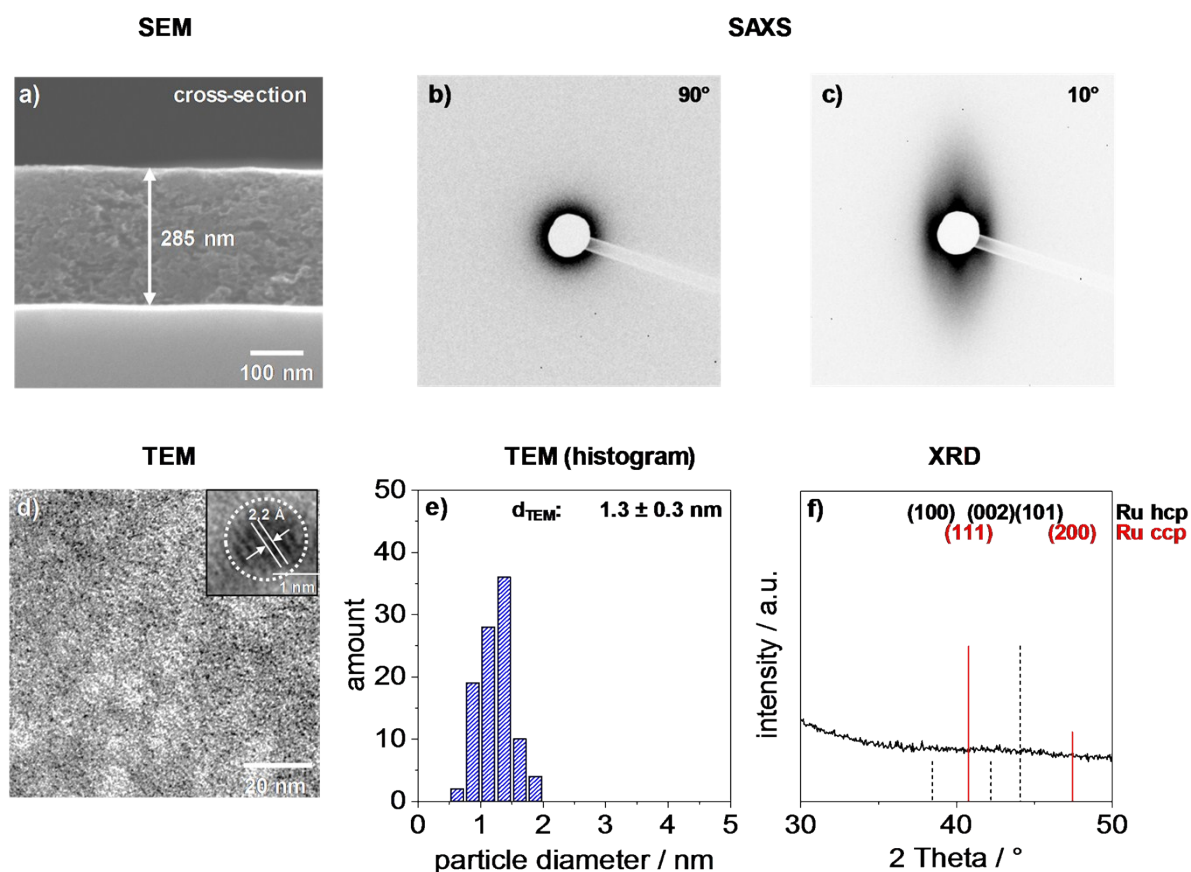
While H₂-treated films show an intact porous carbon structure, a partial collapse of segments of the carbon film can be seen for Ar and N₂ treated samples. The collapse is likely to result from corrosion related to traces of oxygen contained in the deposited material as well as the employed Ar and N₂ gases.



Supplementary Figure S5: SEM images in top-view mode of palladium and platinum-ruthenium nanoparticle containing ordered mesoporous carbon films carbonized at 600 °C and 700 °C for 3h in H₂/Ar-atmosphere (a, d), Ar-atmosphere (b, e) and in N₂-atmosphere (c, f).

SI 6. Morphology and structural properties of RuNP/OMC films

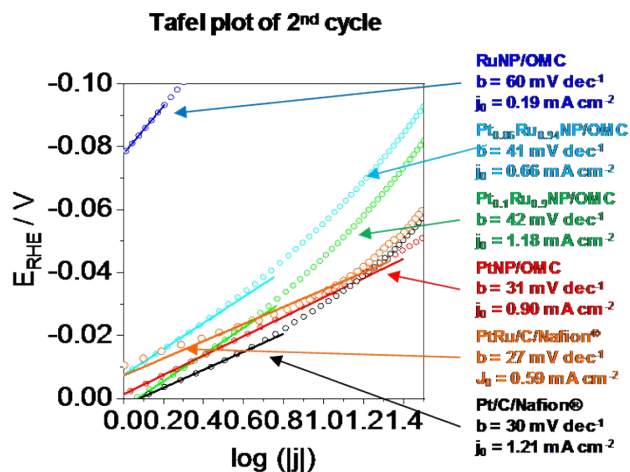
RuNP/OMC films were synthesized by depositing films via dip-coating from a mixture containing a 1,3-dihydroxybenzene-formaldehyde-compound, F127 as a structure directing template and colloidal RuNP in THF. Supplementary figure S6 shows structural features of a RuNP/OMC film carbonized in H₂/Ar atmosphere at 700 °C. A cross-sectional SEM image (S6a) indicates a homogenous film with a thickness of about 285 nm. SAXS measurement in transition mode with a X-ray incident angle of 90° (S6b) as well as recorded in an angle of 10° (S6c) show no pronounced diffraction rings. TEM images (S6d) reveal the presence of small crystalline nanoparticles with regular distance of fringes of 2.2 Å. The average diameter amounts to 1.3 ± 0.3 nm (S6e). A GI-XRD measurement (S6f) shows a weak and broad reflection at ca. 42.2°, which could be an indication of cubic ruthenium. The BET surface area of the RuNP/OMC film amounts to 32 m² m⁻² and the electrical conductivity is 6.5 S cm⁻¹.



Supplementary Figure S6: Morphology of a mesoporous carbon film with integrated ruthenium nanoparticles (5.6 wt%_{Ru}) which was carbonized at 700 °C in H₂/Ar and additionally heat-treated at 300 °C in air and reduced in H₂/Ar at 350 °C. a) cross-sectional SEM image of the RuNP/OMC film indicates a homogenous film with a thickness of 285 nm. SAXS measurement with an angle of incidence of 90° (b) and of 10° (c) indicates no rings. d) TEM image of small RuNPs. A HR-TEM inset indicates regular lattice fringes of 2.2 Å. e) TEM histogram shows monodisperse small nanoparticles with a diameter of 1.3 ± 0.3 nm. f) GI-XRD measurement shows a small broad reflex which is between the main reflexes of Ru hcp and ccp.

SI 7. Tafel evaluation of MeNP/OMC catalyst films

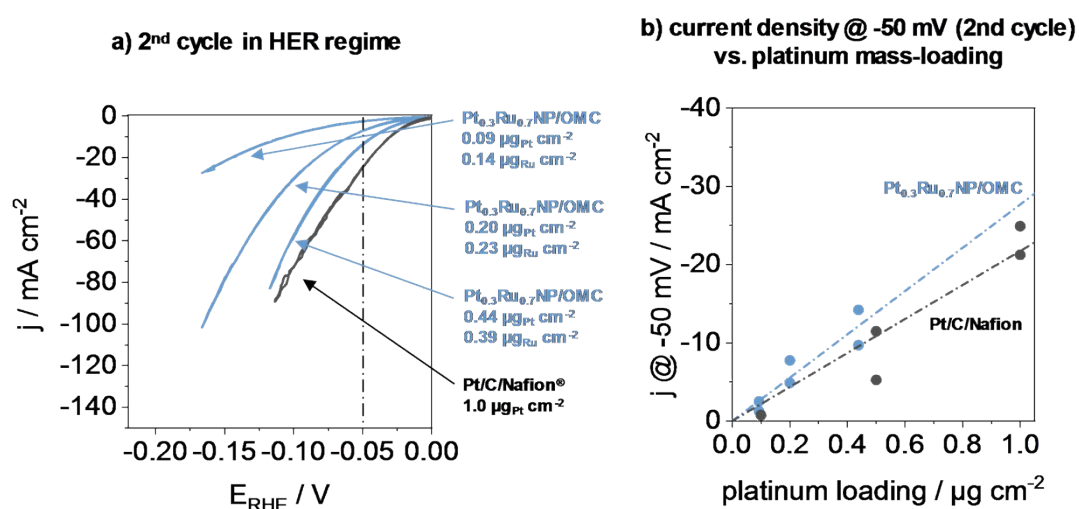
Supplementary figure S7 shows the Tafel-plots of RuNP/OMC, PtNP/OMC, Pt_{0.1}Ru_{0.9}NP/OMC, Pt_{0.06}Ru_{0.94}NP/OMC catalyst films as well as of commercial Pt/C/Nafion® and PtRu/C/Nafion® catalysts.



Supplementary Figure S7: Tafel evaluation of the 2nd cycle (potential E_{RHE} vs. $\log(\text{current density})$), recorded with a scan rate of 20 mV s^{-1} in N_2 -saturated 0.5M sulfuric acid and a rotating speed of 2000 rpm .

SI 8. Electrochemical study of $\text{Pt}_{0.3}\text{Ru}_{0.7}\text{NP}/\text{OMC}$ films with different metal loadings

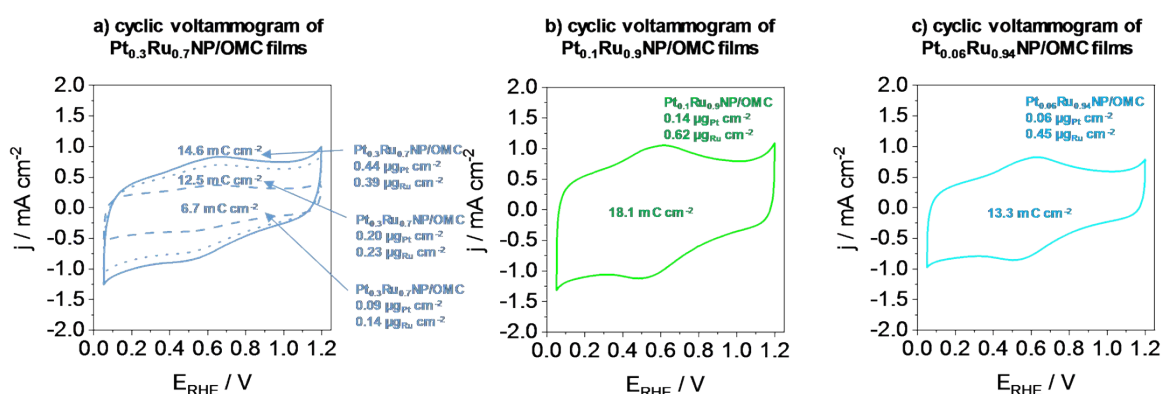
Electrochemical performance of bimetallic $\text{Pt}_{0.3}\text{Ru}_{0.7}\text{NP}/\text{OMC}$ films in the hydrogen evolution reaction. Supplementary figure S8a) shows the current density of the 2nd cycle in the HER regime of 50 mV to -250 mV. S8b) displays the current density of the 2nd cycle at a potential of -50 mV as a function of the geometric platinum loading of $\text{Pt}_{0.3}\text{Ru}_{0.7}\text{NP}/\text{OMC}$ films and Pt/C/Nafion, respectively.



Supplementary Figure S8: Electrocatalytic testing of a $\text{Pt}_{0.3}\text{Ru}_{0.7}\text{NP}/\text{OMC}$ catalyst film series with the same Pt : Ru ratio and different metal loadings. $\text{Pt}_{0.3}\text{Ru}_{0.7}\text{NP}/\text{OMC}$ films carbonized for 3 h under a H_2/Ar atmosphere followed by a subsequent heat-treatment at 300 °C in air and an additionally heat-treatment at 350 °C in H_2/Ar . The shown Pt/C/Nafion® catalyst was prepared by a typical ink-cast procedure. Cyclic voltammograms (CV) were recorded in the HER regime of 50 mV to -250 mV with a scan rate of 20 mV s⁻¹ in 0.5 M sulfuric acid being used as an electrolyte solution. S8a) shows the 2nd cycle and b) the current density at -50 mV as a function of the platinum loading.

SI 9. Basic cyclic voltammetry of PtRuNP/OMC films

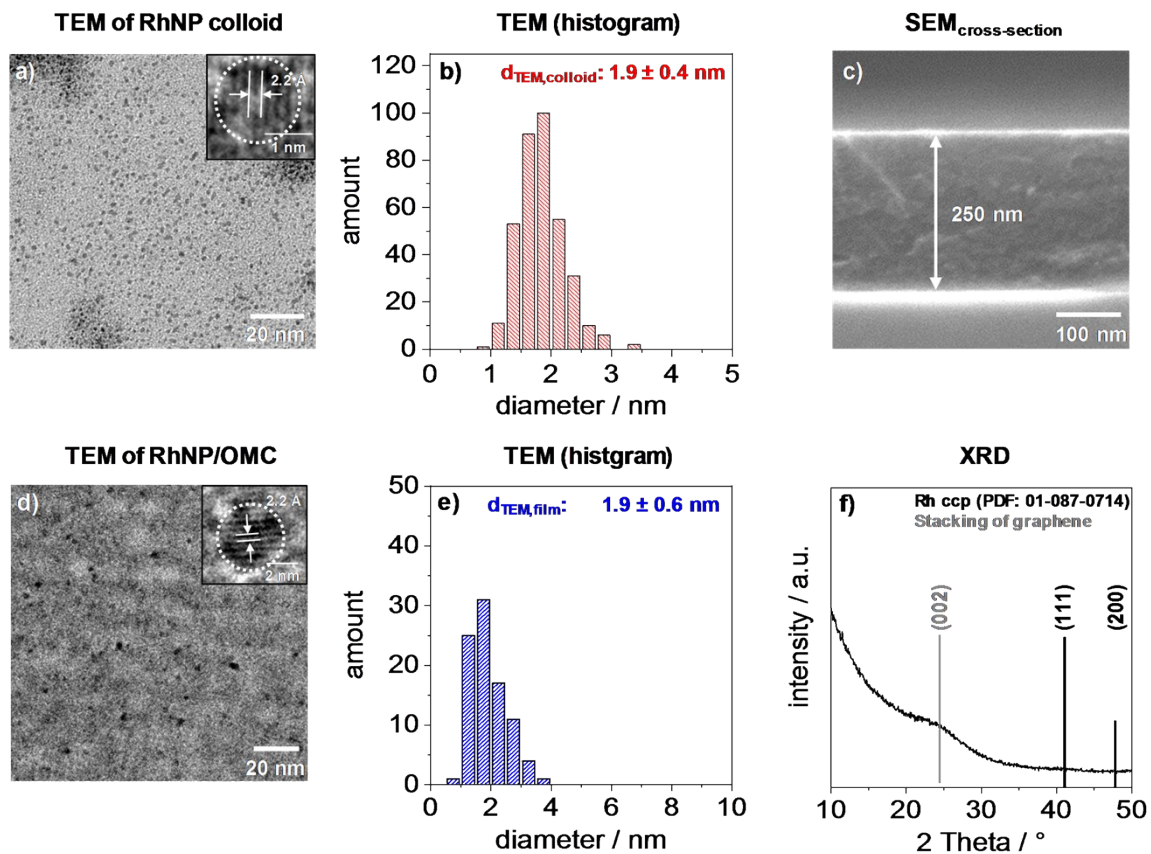
Supplementary Figure S9 shows basic cyclic voltammetry in a range of 0.5 – 1.2 V with a scan rate of 100 mV s⁻¹ for Pt_{0.3}Ru_{0.7}NP/OMC (a), Pt_{0.1}Ru_{0.9}NP/OMC (b) and Pt_{0.06}Ru_{0.94}NP/OMC (c), respectively. The determined capacities are obtained from the integration of the cathodic and anodic charge of the PtRuNP/OMC catalysts. The measured electrochemical surface area is dominated by the capacitive contribution of the carbon, due to the very high surface area of the carbon and the low amount the noble metal nanoparticles.



Supplementary Figure S9: Basic cyclic voltammetry of PtRuNP/OMC catalyst films in a range of 0.5 – 1.2 V and a scan rate of 100 mV s⁻¹. The determined capacities are obtained from the integration of the cathodic and anodic charge of the PtRuNP/OMC catalysts. a) represents the capacities from CV measurements for the series of Pt_{0.3}Ru_{0.7}NP/OMC films, b) for the Pt_{0.1}Ru_{0.9}NP/OMC and c) for the Pt_{0.06}Ru_{0.94}NP/OMC, respectively.

SI 10. Morphology and structural properties of colloidal RhNPs and RhNP/OMC films

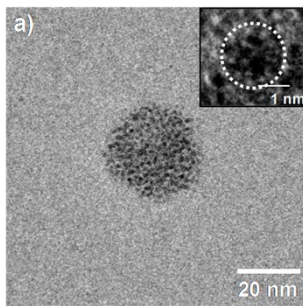
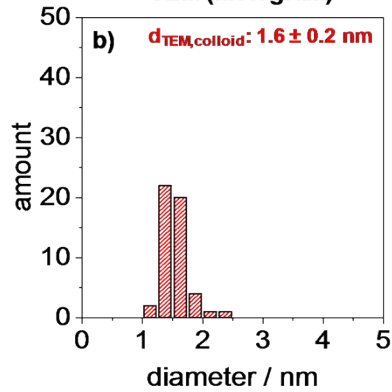
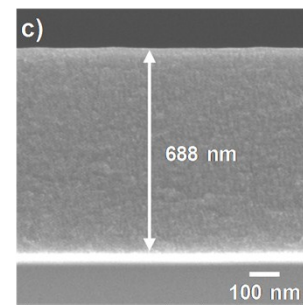
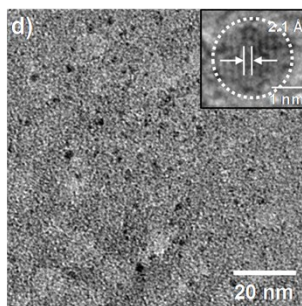
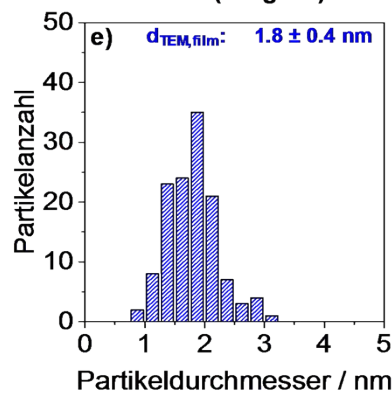
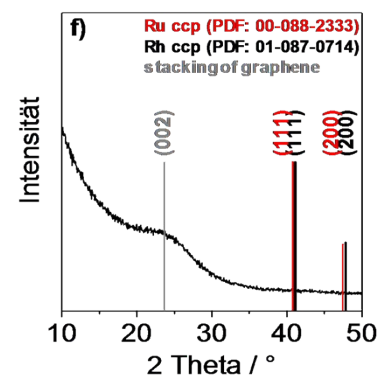
Colloidal Rh nanoparticles were synthesized under argon atmosphere in a glove box ($\text{H}_2\text{O} < 1$ ppm, $\text{O}_2 < 1$ ppm) by adding tetraoctylammonium hydridotriethylborat (0.5 ml) to a suspension composed of 14.8 mg rhodium(III) chloride in THF (8.2 ml). RhNP/OMC films were synthesized by depositing films via dip-coating from a mixture containing a 1,3-dihydroxybenzene-formaldehyde-compound, F127 as a structure directing template and colloidal RhNP in THF. Supplementary figure S10 shows TEM images of the colloidal RhNP and structural features of a RhNP/OMC film carbonized in H_2/Ar atmosphere at 700 °C. TEM images of RhNP (S10a) indicates small particles with an average diameter of 1.9 ± 0.4 nm (S10b) and a high crystallinity with regular lattice fringes of 2.2 Å (HR-TEM inset in S10a). A SEM image in cross-section mode of the RhNP/OMC film indicates a homogenous film with a layer thickness of 250 nm (S10c). TEM images (S10d) reveal small particles which retain their crystallinity (lattice fringes of 2.2 Å) and size (1.9 ± 0.4 nm (e)) during carbonization. GI-XRD measurement (S10f) indicates a small and broad reflection which can be attributed to the (111) plane of Rh. BET surface area of the RhNP/OMC film amounts to $196 \text{ m}^2 \text{ m}^{-2}$ and the electrical conductivity is 9.3 S cm^{-2} . The geometric loading was determined by WDX/StrataGem and the Rh-loading amounts to $0.8 \text{ } \mu\text{g cm}^{-2}$.



Supplementary figure S10: Characterization of colloidal RhNP and RhNP/OMC film carbonized at 700 °C in H₂/Ar. a) TEM image of small colloidal RhNP. HR-TEM inset indicates regular lattice fringes of 2.2 Å. b) TEM histogram shows monodisperse small nanoparticles with a diameter of 1.9 ± 0.4 nm. c) cross-section SEM image of a RhNP/OMC film reveals a homogenous film with a thickness of 250 nm. d) TEM images of the nanoparticle indicate that the particles retain their size (1.9 ± 0.4 nm (e)) and crystallinity (lattice fringes of 2.2 Å (d inset)) when incorporated in a film. f) GI-XRD measurement shows a small broad reflex which can be attributed to the (111) plane of Rh.

SI 11. Morphology and structural properties of colloidal RhRuNPs and RhRuNP/OMC films

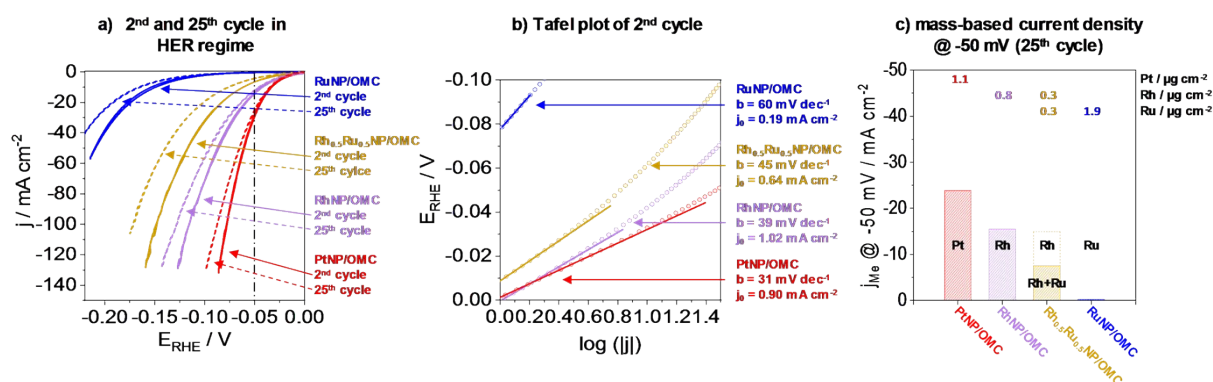
Colloidal RhRu nanoparticles were synthesized under argon atmosphere in a glove box ($\text{H}_2\text{O} < 1$ ppm, $\text{O}_2 < 1$ ppm) by adding tetraoctylammonium hydridotriethylborat (0.5 ml) to a suspension composed of 7.42 mg rhodium(III) chloride and 7.22 mg ruthenium(III) chloride (metal ratio Rh : Ru = 0.5 : 0.5) in THF (8.9 ml). RhRuNP/OMC films were synthesized by depositing films via dip-coating from a mixture containing a 1,3-dihydroxybenzene-formaldehyde-compound, F127 as a structure directing template and colloidal RhRuNP in THF. Supplementary figure S11 shows TEM images of the colloidal RhRuNP and structural features of a RhRuNP/OMC film carbonized in H_2/Ar atmosphere at 700 °C. TEM images of RhRuNP (S11a) indicates small particles within a particle cluster. The average diameter of the particles amounts to 1.6 ± 0.2 nm (S11b) and a HR-TEM inset in S11a indicates no lattice fringes. A SEM image in cross-section mode (S11c) of the RhRuNP/OMC film indicates a homogenous film with a layer thickness of 688 nm. TEM images (S11d) reveal small particles with a high crystallinity (lattice fringes of 2.1 Å) and a particle size of 1.8 ± 0.4 nm (S11e). GI-XRD measurement (S11f) indicates no distinct reflection for Rh and Ru. The BET surface area of the RhRuNP/OMC film amounts to $338 \text{ m}^2 \text{ m}^{-2}$ and the electrical conductivity is 3.1 S cm^{-2} . The geometric loading amounts to $0.3 \mu\text{g cm}^{-2}$ for Rh and $0.3 \mu\text{g cm}^{-2}$ for Ru.

TEM of RhRuNP colloid**TEM (histogram)****SEM_{cross-section}****TEM of RhRuNP/OMC****TEM (histogram)****XRD**

Supplementary Figure S11: Characterization of colloidal RhRuNP and RhRuNP/OMC film carbonized at 700 °C in H₂/Ar. a) TEM image of small colloid RhRuNP. HR-TEM inset indicates no regular lattice fringes. b) TEM histogram shows monodisperse small nanoparticles with a diameter of 1.6 ± 0.2 nm. c) cross-section SEM image of a RhRuNP/OMC film reveals a homogenous film with a thickness of 688 nm. d) TEM images of the nanoparticles implemented in an OMC. e) indicates that the particles retain their size (1.8 ± 0.4 nm) and show a high crystallinity (lattice fringes of 2.1 Å (d inset)) after carbonization. f) GI-XRD measurement shows no distinct reflection for Rh and Ru.

SI 12. Electrochemical testing of RhNP/OMC and RhRuNP/OMC catalyst films in the HER regime

Electrochemical performance of RhNP/OMC and RhRuNP/OMC catalyst films in the HER regime was studied in a three-electrode rotating disc setup by using a coated GC disk as working electrode, a Pt gauze as counter electrode and a RHE as reference electrode. 0.5M H₂SO₄ was used as electrolyte. Supplementary figure S12a shows the 2nd and 25th cycle of cyclic voltammetry measurements. Supplementary figure S12b displays the Tafel evaluation of the films and S12c exhibit the mass-based current density at a potential of -50 mV. PtNP/OMC und RuNP/OMC catalyst films are shown for comparison. RhNP/OMC and RhRuNP/OMC catalysts exhibit values of -14.6 mA cm⁻² and -7.1 mA cm⁻² in the 2nd CV at an overpotential of -50 mV for RhNP/OMC and RhRuNP/OMC, respectively. After the 25th cycle catalyst films show a decreasing of 15.4% for the RhNP/OMC (-12.46 mA cm⁻²) and of 37.1% for the RhRuNP/OMC (-4.56 mA cm⁻²). Tafel evaluation (S12b) of the 2nd cycle shows for both catalysts a similar Tafel slope of about 40 mV dec⁻¹ which indicates a limitation induced by the electrochemical desorption of H₂ from the active electrocatalytic center (Heyrovsky reaction, $H_{ads} + H^+ + e^- \rightleftharpoons H_2$). The exchange current density of the RhNP/OMC amounts to 1.02 mA cm⁻² and shows a similar value as PtNP/OMC. The bimetallic RhRuNP/OMC exhibit an exchange current density value of 0.64 mA cm⁻². S12c compares the mass-based current density at a potential of -50 mV of the 25th cycle during CV. RhNP/OMC reaches a mass-based current density of -15.5 mA μg_{Rh}⁻¹ and RhRuNP/OMC shows a value of -7.5 mA μg_{Rh+Ru}⁻¹ for the total metal content of Rh and Ru. The mass-based current density referred to Rh amounts to -14.9 mA μg_{Rh}⁻¹ and thus has similar value as the monometallic RhNP/OMC.



Supplementary Figure S12: The electrocatalytic performance is illustrated for RhNP/OMC and RhRuNP/OMC catalysts films and a PtNP/OMC as well as RuNP/OMC catalyst films for comparison. MeNP/OMC films carbonized for 3 h under a H₂/Ar atmosphere followed by a subsequent heat-treatment at 300 °C in air and an additionally heat-treatment at 350 °C in H₂/Ar. Cyclic voltammograms (CV) were recorded in the HER regime of 50 mV to -250 mV with a scan rate of 20 mV s⁻¹ in 0.5M sulfuric acid being used as an electrolyte solution. a) shows the 2nd and 25th cycle. b) displays the Tafel evaluation of the MeNP/OMC films and c) shows the measured current density at -50 mV from the 25th CV.

References

- [1] C. Boissiere, D. Grosso, S. Lepoutre, L. Nicole, A. B. Bruneau, C. Sanchez, *Langmuir* 2005, 21, 12362-12371.